PANE Journal of Physics Education P. J. Phys. Edu. Vol 1(2), October 2026

RELATIVISTIC DYNAMICS OF SIMPLE AND COUPLED DOUBLE PENDULUMS

Mang Semi Subba[1], Arghya Mukherjee[2], and Rupak Mukherjee[*1]

[1]*Department of Physics, Sikkim University, Gangtok 737102, Sikkim, India*
[2]*Department of Physics, Amity University, Punjab, India*

[*]Corresponding Author: rmukherjee@cus.ac.in

Abstract: The double pendulum is one of the most widely studied systems in classical mechanics because of its rich nonlinear behaviour and its importance in understanding coupled oscillations and deterministic chaos. While its classical dynamics are well established, relativistic extensions have received comparatively little attention. In this work, we develop a relativistic formulation of both the simple and coupled double pendulum within the framework of special relativity using the Lagrangian formalism. Starting from the physical model, the equations of motion are derived by incorporating the relativistic kinetic energy while retaining the classical gravitational potential. The resulting nonlinear equations are transformed into an equivalent first-order state-space system and solved numerically using the classical fourth-order Runge–Kutta method. Numerical simulations are carried out in dimensionless form for small-angle in-phase motion, small-angle out-of-phase motion, and large-angle nonlinear motion. Time evolution, phase-space trajectories, and Lorentz factors are examined to investigate the influence of relativistic effects on the system dynamics. The results show that the relativistic formulation naturally reproduces the classical behaviour in the low-velocity limit while introducing velocity-dependent corrections that become increasingly significant as the system approaches relativistic speeds. Besides extending a familiar nonlinear system into the relativistic regime, the present formulation provides a self-contained example that brings together Lagrangian mechanics, special relativity, and numerical methods within a single framework, making it a useful reference for advanced studies in classical and computational mechanics.

Keywords: relativistic dynamics; double pendulum; Lagrangian mechanics; nonlinear dynamics; phase-space analysis; numerical simulation

(Received: 31 July 2026; accepted: 11 October 2026; published: 30 October 2026)

1 Introduction

Pendulum systems have long been used as important models in classical mechanics because they provide a simple way to study oscillatory motion, analytical mechanics, and nonlinear dynamics. Despite their apparent simplicity, pendulums exhibit a wide range of physical behaviour, making them useful for investigating periodic motion, resonance, stability, and nonlinear oscillations. While the simple pendulum has been studied extensively for many years, the coupled double pendulum displays much richer dynamics due to the interaction between its two degrees of freedom. For this reason, pendulum systems continue to be widely used as benchmark models in theoretical physics, applied mechanics, and computational studies [1–3].

The motion of a simple pendulum remains regular under ideal conditions, whereas the coupled double pendulum can exhibit highly nonlinear behaviour and even deterministic chaos for suitable initial conditions. One of the key features of chaotic motion is its sensitive dependence on initial conditions, where two trajectories starting from nearly identical states separate rapidly with time despite being governed by deterministic equations. Because of these characteristics, the double pendulum has become one of the most widely studied systems for understanding nonlinear dynamics, phase-space behaviour, and chaos in classical mechanics [4–6].

The classical double pendulum has been investigated using analytical, numerical, and experimental methods. Levien and Tan presented a detailed study of the double pendulum using the Lagrangian approach and demonstrated

its nonlinear behaviour through both theoretical and experimental analysis [7]. Shinbrot *et al.* experimentally confirmed the chaotic nature of the system and highlighted its strong sensitivity to initial conditions [6]. More recently, D'Alessio carried out a combined analytical, numerical, and experimental study of both the simple and double pendulum, showing that modern computational methods can successfully reproduce their complex dynamics [8]. These studies have helped establish the double pendulum as one of the standard models for investigating nonlinear mechanical systems.

Although classical mechanics describes pendulum motion accurately under ordinary conditions, relativistic effects become important when the velocities of the masses approach a significant fraction of the speed of light. In this regime, the classical relationships between momentum, energy, and velocity are no longer sufficient, and relativistic corrections must be included. The Lagrangian formulation provides a convenient and consistent framework for incorporating these corrections while preserving the variational formulation of the equations of motion [1, 2, 9].

Compared with the large amount of work available on the classical double pendulum, relatively few studies have considered relativistic effects in coupled nonlinear pendulum systems. Investigating how relativistic corrections influence the motion of a coupled double pendulum is therefore of theoretical interest. Such a study helps extend one of the most familiar nonlinear mechanical systems into the relativistic regime and provides further insight into the combined effects of relativity and nonlinear dynamics.

In this work, the relativistic dynamics of both the simple pendulum and the coupled double pendulum are investigated using analytical and numerical methods. The classical equations of motion are first reviewed to establish the mathematical framework, after which the corresponding relativistic equations are derived using the Lagrangian formalism. The resulting nonlinear equations are solved numerically using the classical fourth-order Runge–Kutta method. The effects of relativity are then examined through the time evolution of the angular coordinates and their corresponding phase-space trajectories. Finally, comparisons between the classical and relativistic models are presented to illustrate how relativistic corrections modify the overall dynamical behaviour of the systems.

The remainder of this paper is organized as follows. Section 2 presents the mathematical formulation of the classical and relativistic pendulum models. Section 3 describes the numerical method used to solve the governing equations. Section 4 presents and discusses the numerical results for both the simple and coupled double pendulum. Finally, Section 5 summarizes the main conclusions of this work.

2 Mathematical Formulation

This section presents the mathematical formulation of the simple and coupled double pendulum considered in this work. The classical models are first reviewed to establish the notation and governing equations used throughout the paper. These formulations are then extended to include relativistic effects, providing the foundation for the numerical analysis presented in the subsequent sections.

2.1 Classical Simple Pendulum

The simple pendulum consists of a point mass m suspended from a fixed pivot by a rigid, massless rod of length L. The motion is confined to a vertical plane and is described by the generalized coordinate θ. Within the framework of classical mechanics, the dynamics are conveniently formulated using the Lagrangian approach, which also provides the foundation for the relativistic extension developed in the following subsection [1–3].

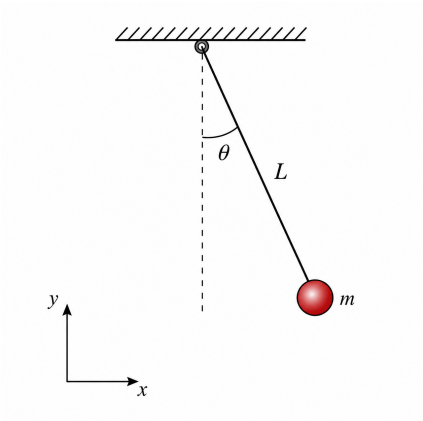


Figure 1: Schematic illustration of the classical simple pendulum showing the bob mass m, rod length L, and angular displacement θ measured from the downward vertical. The figure is provided to illustrate the geometry and notation used in this work.

For a pendulum moving along a circular arc, the kinetic and potential energies are

$$T = \frac{1}{2}mL^2\dot{\theta}^2, \tag{1}$$

$$V = mgL\left(1 - \cos\theta\right), \tag{2}$$

respectively, giving the classical Lagrangian

$$\mathcal{L} = \frac{1}{2}mL^2\dot{\theta}^2 - mgL\left(1 - \cos\theta\right). \tag{3}$$

Applying the Euler–Lagrange equation,

$$\frac{d}{dt}\left(\frac{\partial\mathcal{L}}{\partial\dot{\theta}}\right) - \frac{\partial\mathcal{L}}{\partial\theta} = 0, \tag{4}$$

yields the familiar nonlinear equation of motion,

$$\ddot{\theta} + \frac{g}{L}\sin\theta = 0. \tag{5}$$

In the small-angle limit, $\sin\theta \approx \theta$, Eq. (5) reduces to

$$\ddot{\theta} + \omega_0^2\theta = 0, \tag{6}$$

where

$$\omega_0 = \sqrt{\frac{g}{L}} \tag{7}$$

is the natural angular frequency of the pendulum. The classical formulation presented above serves as the reference model for the relativistic extension developed in the following subsection.

2.2 Relativistic Simple Pendulum

Classical mechanics provides an accurate description of pendulum motion when the velocity of the bob is much smaller than the speed of light. As the velocity approaches relativistic values, however, the classical relationship between momentum and velocity is no longer valid, and the dynamics must be described within the framework of special relativity. The Lagrangian formalism provides a natural extension of the classical formulation while preserving the variational structure of the equations of motion [1, 2, 9].

Consider a simple pendulum consisting of a point mass m suspended from a fixed pivot by a rigid, massless rod of length L. The motion is confined to a vertical plane and is described by the generalized coordinate θ. Since the bob moves along a circular arc, its speed is given by $v = L\dot{\theta}$.

The relativistic Lagrangian of the system is

$$\mathcal{L} = -mc^2\sqrt{1 - \frac{L^2\dot{\theta}^2}{c^2}} - mgL\left(1 - \cos\theta\right), \tag{8}$$

where the first term represents the relativistic kinetic energy and the second term corresponds to the gravitational potential energy.

Applying the Euler–Lagrange equation,

$$\frac{d}{dt}\left(\frac{\partial\mathcal{L}}{\partial\dot{\theta}}\right) - \frac{\partial\mathcal{L}}{\partial\theta} = 0, \tag{9}$$

yields the relativistic equation of motion,

$$\ddot{\theta} + \frac{g}{L}\left(1 - \frac{L^2\dot{\theta}^2}{c^2}\right)^{3/2}\sin\theta = 0, \tag{10}$$

which governs the nonlinear motion of the relativistic simple pendulum. In contrast to the classical equation, the restoring force is modified by a velocity-dependent relativistic factor, introducing an additional nonlinear coupling between the angular displacement and angular velocity. As a result, the oscillatory motion deviates progressively from the classical prediction with increasing velocity.

In the non-relativistic limit,

$$\frac{L\dot{\theta}}{c} \ll 1, \tag{11}$$

Eq. (10) reduces to

$$\ddot{\theta} + \frac{g}{L}\sin\theta = 0, \tag{12}$$

recovering the classical equation of motion and thereby confirming the consistency of the relativistic formulation.

2.3 Classical Coupled Double Pendulum

The coupled double pendulum consists of two point masses, m_1 and m_2, connected by rigid, massless rods of lengths L_1 and L_2, respectively. The motion is confined to a vertical plane and is described by the generalized coordinates θ_1 and θ_2, measured from the downward vertical. Owing to its two degrees of freedom and nonlinear coupling, the system exhibits a wide range of dynamical behaviour, including periodic, quasi-periodic, and chaotic motion depending on the initial conditions [4, 6, 7].

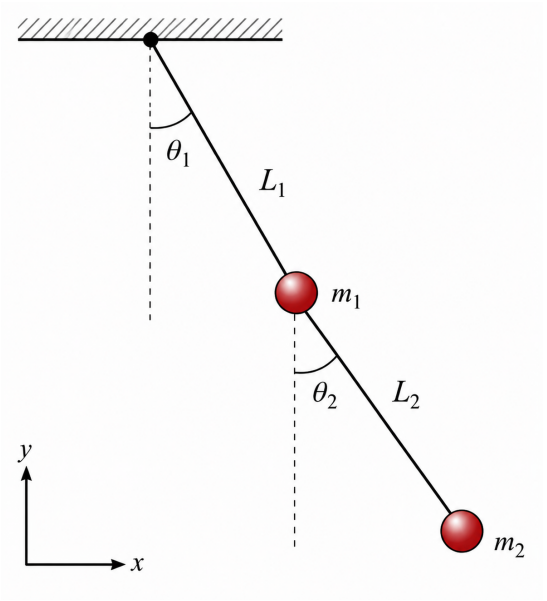


Figure 2: Schematic representation of the classical coupled double pendulum showing the masses m_1 and m_2, rod lengths L_1 and L_2, and angular coordinates θ_1 and θ_2 measured from the downward vertical. This figure is intended for illustration of the system geometry only.

The Cartesian coordinates of the two masses are

$$x_1 = L_1 \sin\theta_1, \qquad y_1 = -L_1 \cos\theta_1, \tag{13}$$

$$x_2 = L_1 \sin\theta_1 + L_2 \sin\theta_2, \qquad y_2 = -L_1 \cos\theta_1 - L_2 \cos\theta_2. \tag{14}$$

Differentiating the position coordinates with respect to time gives the velocity components, from which the kinetic and potential energies are obtained as

$$T = \frac{1}{2}(m_1 + m_2)L_1^2\dot{\theta}_1^2 + \frac{1}{2}m_2 L_2^2\dot{\theta}_2^2 + m_2 L_1 L_2 \dot{\theta}_1\dot{\theta}_2 \cos(\theta_1 - \theta_2), \tag{15}$$

and

$$V = -(m_1 + m_2)gL_1 \cos\theta_1 - m_2 g L_2 \cos\theta_2, \tag{16}$$

respectively. The corresponding classical Lagrangian is therefore

$$\mathcal{L} = T - V. \tag{17}$$

Application of the Euler–Lagrange equations,

$$\frac{d}{dt}\left(\frac{\partial \mathcal{L}}{\partial \dot{\theta}_i}\right) - \frac{\partial \mathcal{L}}{\partial \theta_i} = 0, \qquad (i = 1, 2), \tag{18}$$

yields the coupled nonlinear equations governing the classical double pendulum. Since these equations are well established in the literature, they are not reproduced here and the reader is referred to Refs. [7, 8] for their complete derivation.

The classical formulation presented above establishes the notation and analytical framework employed in the relativistic extension developed in the following subsection.

2.4 Relativistic Coupled Double Pendulum

2.4.1 Physical Model

The coupled double pendulum is a well-known mechanical system that exhibits complex nonlinear behaviour because of the interaction between its two degrees of freedom. While its classical dynamics have been studied extensively, including relativistic effects introduces additional velocity-dependent terms that modify the equations of motion.

In this work, we consider a planar double pendulum consisting of two point masses, m_1 and m_2, connected by rigid, massless rods of lengths l_1 and l_2, respectively. The first pendulum is suspended from a fixed pivot, and the second mass is attached to the end of the first rod. The motion of the system is described by the generalized coordinates $\theta_1(t)$ and $\theta_2(t)$, measured from the downward vertical.

The Cartesian coordinates of the two masses are

$$x_1 = l_1 \sin\theta_1, \qquad y_1 = -l_1 \cos\theta_1, \tag{19}$$

$$x_2 = l_1 \sin\theta_1 + l_2 \sin\theta_2, \qquad y_2 = -l_1 \cos\theta_1 - l_2 \cos\theta_2. \tag{20}$$

The equations of motion are obtained using the Lagrangian formalism,

$$\mathcal{L} = T - V, \tag{21}$$

where the classical kinetic energy is replaced by its relativistic expression, while the gravitational potential energy remains unchanged. This introduces velocity-dependent Lorentz factors into the equations of motion, leading to additional nonlinear coupling between the two pendulum arms. When the velocities are much smaller than the speed of light, the relativistic formulation reduces to the corresponding classical model.

The following assumptions are made throughout this work:

- The masses are treated as point particles.
- The rods are rigid and massless.
- The motion is restricted to a single vertical plane.
- Frictional and air resistance effects are neglected.
- No external driving force acts on the system.

Under these assumptions, the system is conservative, and its motion is governed only by gravity and the coupling between the two pendulum arms. The kinematic relations presented above provide the starting point for deriving the relativistic equations of motion.

2.4.2 Geometry and Kinematics

The motion of the coupled double pendulum is conveniently described using the generalized coordinates $\theta_1(t)$ and $\theta_2(t)$, measured from the downward vertical. The corresponding Cartesian coordinates of the two masses are

$$x_1 = L_1 \sin\theta_1, \qquad y_1 = -L_1 \cos\theta_1, \tag{22}$$

$$x_2 = L_1 \sin\theta_1 + L_2 \sin\theta_2, \qquad y_2 = -L_1 \cos\theta_1 - L_2 \cos\theta_2. \tag{23}$$

Differentiating the above expressions with respect to time gives the velocity components of the two masses. Consequently, the squared speed of the first mass is

$$v_1^2 = L_1^2\dot{\theta}_1^2, \tag{24}$$

while the squared speed of the second mass is

$$v_2^2 = L_1^2\dot{\theta}_1^2 + L_2^2\dot{\theta}_2^2 + 2L_1L_2\dot{\theta}_1\dot{\theta}_2\cos(\theta_1 - \theta_2). \tag{25}$$

These expressions form the kinematic basis for constructing the relativistic kinetic energy of the coupled double pendulum in the following subsection.

2.4.3 Relativistic Kinetic and Potential Energy

The relativistic formulation differs from the classical model only through the kinetic energy. For a free particle of mass m moving with speed v, the relativistic Lagrangian is

$$L_{\text{free}} = -mc^2\sqrt{1 - \frac{v^2}{c^2}}, \tag{26}$$

which reduces to the classical kinetic energy in the low-velocity limit.

The total relativistic kinetic energy of the coupled double pendulum is therefore

$$T = -m_1c^2\sqrt{1 - \frac{v_1^2}{c^2}} - m_2c^2\sqrt{1 - \frac{v_2^2}{c^2}}, \tag{27}$$

where the squared speeds v_1^2 and v_2^2 are given by Eqs. (24) and (25), respectively. Substituting these expressions yields

$$\begin{aligned} T = &- m_1c^2\sqrt{1 - \frac{L_1^2\dot{\theta}_1^2}{c^2}} \\ &- m_2c^2\sqrt{1 - \frac{L_1^2\dot{\theta}_1^2 + L_2^2\dot{\theta}_2^2 + 2L_1L_2\dot{\theta}_1\dot{\theta}_2\cos(\theta_1 - \theta_2)}{c^2}}. \end{aligned} \tag{28}$$

Equation (28) contains the complete relativistic coupling between the two pendulum arms through the velocity-dependent square-root terms.

The gravitational potential energy retains its classical form and is given by

$$V = -(m_1 + m_2)gL_1\cos\theta_1 - m_2gL_2\cos\theta_2. \tag{29}$$

2.4.4 Construction and Normalization of the Relativistic Lagrangian

The relativistic Lagrangian of the coupled double pendulum is obtained by combining the relativistic kinetic energy given by Eq. (28) with the gravitational potential energy of Eq. (29). Thus,

$$\begin{aligned}\mathcal{L} = &- m_1 c^2 \sqrt{1 - \frac{L_1^2 \dot{\theta}_1^2}{c^2}} \\ &- m_2 c^2 \sqrt{1 - \frac{L_1^2 \dot{\theta}_1^2 + L_2^2 \dot{\theta}_2^2 + 2 L_1 L_2 \dot{\theta}_1 \dot{\theta}_2 \cos(\theta_1 - \theta_2)}{c^2}} \\ &+ (m_1 + m_2) g L_1 \cos\theta_1 + m_2 g L_2 \cos\theta_2. \end{aligned} \tag{30}$$

Equation (30) constitutes the complete relativistic Lagrangian of the planar coupled double pendulum and forms the basis for the derivation of the governing equations of motion.

For numerical implementation, it is convenient to express the Lagrangian in dimensionless form. Dividing Eq. (30) by the characteristic energy scale $m_1 c^2$ and introducing the mass ratio

$$\mu = \frac{m_2}{m_1}, \tag{31}$$

together with the dimensionless angular velocities

$$\bar{\theta}_1 = \frac{L_1 \dot{\theta}_1}{c}, \qquad \bar{\theta}_2 = \frac{L_2 \dot{\theta}_2}{c}, \tag{32}$$

and the dimensionless gravitational parameters

$$\alpha_1 = \frac{g L_1}{c^2}, \qquad \alpha_2 = \frac{g L_2}{c^2}, \tag{33}$$

the normalized Lagrangian becomes

$$\begin{aligned}\tilde{\mathcal{L}} = &- \sqrt{1 - \bar{\theta}_1^2} \\ &- \mu \sqrt{1 - \bar{\theta}_1^2 - \bar{\theta}_2^2 - 2 \bar{\theta}_1 \bar{\theta}_2 \cos(\theta_1 - \theta_2)} \\ &+ (1 + \mu) \alpha_1 \cos\theta_1 + \mu \alpha_2 \cos\theta_2. \end{aligned} \tag{34}$$

Equation (34) is the dimensionless relativistic Lagrangian employed throughout the remainder of this work. The corresponding equations of motion are obtained in the following subsection using the Euler–Lagrange formalism.

2.4.5 Euler–Lagrange Equations and Generalized Momenta

The equations of motion are obtained from the normalized Lagrangian, Eq. (34), by applying the Euler–Lagrange equations,

$$\frac{d}{dt}\left(\frac{\partial \tilde{\mathcal{L}}}{\partial \dot{q}_i}\right) - \frac{\partial \tilde{\mathcal{L}}}{\partial q_i} = 0, \qquad (q_i = \theta_1, \theta_2). \tag{35}$$

To simplify the resulting expressions, the relativistic Lorentz factors are introduced as

$$\gamma_1 = \frac{1}{\sqrt{1 - \bar{\theta}_1^2}}, \tag{36}$$

and

$$\gamma_2 = \frac{1}{\sqrt{1 - \bar{\theta}_1^2 - \bar{\theta}_2^2 - 2\bar{\theta}_1\bar{\theta}_2\cos(\theta_1 - \theta_2)}}. \tag{37}$$

The generalized momenta are defined by

$$P_i = \frac{\partial \tilde{\mathcal{L}}}{\partial \bar{\theta}_i}, \qquad (i = 1, 2). \tag{38}$$

Differentiating the normalized Lagrangian with respect to $\bar{\theta}_1$ gives

$$P_1 = \bar{\theta}_1\gamma_1 + \mu\left(\bar{\theta}_1 + \bar{\theta}_2\cos(\theta_1 - \theta_2)\right)\gamma_2. \tag{39}$$

Similarly,

$$P_2 = \mu\left(\bar{\theta}_2 + \bar{\theta}_1\cos(\theta_1 - \theta_2)\right)\gamma_2. \tag{40}$$

The generalized momenta given by Eqs. (39) and (40) incorporate the relativistic coupling between the two pendulum arms through the Lorentz factors and constitute the fundamental dynamical variables employed in the subsequent derivation of the governing equations.

2.4.6 Evaluation of the Generalized Forces

Having obtained the generalized momenta, the remaining quantities required in the Euler–Lagrange equations are the generalized forces,

$$F_i = \frac{\partial \tilde{\mathcal{L}}}{\partial \theta_i}, \qquad (i = 1, 2), \tag{41}$$

where $\tilde{\mathcal{L}}$ is the normalized Lagrangian given by Eq. (34). Since the first relativistic kinetic term depends only on the generalized velocity $\bar{\theta}_1$, it does not contribute to the coordinate derivatives. Consequently, only the second relativistic kinetic term and the gravitational potential contribute to the generalized forces.

Evaluation of F_1 Differentiating the second kinetic term with respect to θ_1 gives

$$\frac{\partial}{\partial \theta_1}\left(-\mu\sqrt{1 - \bar{\theta}_1^2 - \bar{\theta}_2^2 - 2\bar{\theta}_1\bar{\theta}_2\cos(\theta_1 - \theta_2)}\right). \tag{42}$$

Applying the chain rule,

$$\begin{aligned} &= -\mu\frac{1}{2\sqrt{1 - \bar{\theta}_1^2 - \bar{\theta}_2^2 - 2\bar{\theta}_1\bar{\theta}_2\cos(\theta_1 - \theta_2)}} \\ &\quad \times \frac{\partial}{\partial \theta_1}\left[1 - \bar{\theta}_1^2 - \bar{\theta}_2^2 - 2\bar{\theta}_1\bar{\theta}_2\cos(\theta_1 - \theta_2)\right]. \end{aligned} \tag{43}$$

Since

$$\frac{\partial}{\partial \theta_1}\cos(\theta_1 - \theta_2) = -\sin(\theta_1 - \theta_2), \tag{44}$$

we obtain

$$\frac{\partial}{\partial\theta_1}\left[1-\bar{\theta}_1^2-\bar{\theta}_2^2-2\bar{\theta}_1\bar{\theta}_2\cos(\theta_1-\theta_2)\right]=2\bar{\theta}_1\bar{\theta}_2\sin(\theta_1-\theta_2). \tag{45}$$

Hence,

$$\frac{\partial}{\partial\theta_1}(\text{kinetic term})=-\mu\bar{\theta}_1\bar{\theta}_2\sin(\theta_1-\theta_2)\gamma_2. \tag{46}$$

The gravitational contribution is

$$\frac{\partial}{\partial\theta_1}\left[(1+\mu)\alpha_1\cos\theta_1\right]=-(1+\mu)\alpha_1\sin\theta_1. \tag{47}$$

Combining both contributions gives

$$F_1=-\mu\bar{\theta}_1\bar{\theta}_2\sin(\theta_1-\theta_2)\gamma_2-(1+\mu)\alpha_1\sin\theta_1. \tag{48}$$

Evaluation of F_2 Proceeding similarly,

$$\begin{aligned}\frac{\partial}{\partial\theta_2}(\text{kinetic term})&=-\mu\frac{1}{2\sqrt{\cdots}}\frac{\partial}{\partial\theta_2}\left[1-\bar{\theta}_1^2-\bar{\theta}_2^2-2\bar{\theta}_1\bar{\theta}_2\cos(\theta_1-\theta_2)\right]\\&=\mu\bar{\theta}_1\bar{\theta}_2\sin(\theta_1-\theta_2)\gamma_2.\end{aligned} \tag{49}$$

The gravitational contribution is

$$\frac{\partial}{\partial\theta_2}\left(\mu\alpha_2\cos\theta_2\right)=-\mu\alpha_2\sin\theta_2. \tag{50}$$

Therefore,

$$F_2=\mu\bar{\theta}_1\bar{\theta}_2\sin(\theta_1-\theta_2)\gamma_2-\mu\alpha_2\sin\theta_2. \tag{51}$$

The generalized forces given by Eqs. (48) and (51) contain equal and opposite coupling terms arising from the relativistic interaction between the two pendulum arms. Together with the generalized momenta derived previously, these quantities complete the Euler–Lagrange formulation of the relativistic coupled double pendulum.

2.4.7 Evaluation of the Coefficient Matrix

The Euler–Lagrange equations may be written in the compact form

$$\frac{dP_1}{dt}=F_1,\qquad\frac{dP_2}{dt}=F_2. \tag{52}$$

Since the generalized momenta depend on both the generalized coordinates and generalized velocities, their total time derivatives contain acceleration terms. To isolate these accelerations, we evaluate the derivatives of the generalized momenta with respect to the generalized velocities. The resulting quantities form the coefficients of the inertia matrix,

$$A=\frac{\partial P_1}{\partial\bar{\theta}_1},\qquad B=\frac{\partial P_1}{\partial\bar{\theta}_2}, \tag{53}$$

$$D = \frac{\partial P_2}{\partial \bar{\theta}_1}, \qquad E = \frac{\partial P_2}{\partial \bar{\theta}_2}. \tag{54}$$

Evaluation of $A = \partial P_1/\partial \bar{\theta}_1$ Starting from Eq. (39),

$$P_1 = \bar{\theta}_1 \gamma_1 + \mu \left(\bar{\theta}_1 + \bar{\theta}_2 \cos \Delta\theta\right) \gamma_2, \tag{55}$$

the derivative is obtained using the product rule.

For the first term,

$$\frac{\partial}{\partial \bar{\theta}_1}(\bar{\theta}_1 \gamma_1) = \gamma_1 + \bar{\theta}_1 \frac{\partial \gamma_1}{\partial \bar{\theta}_1}, \tag{56}$$

where

$$\frac{\partial \gamma_1}{\partial \bar{\theta}_1} = \bar{\theta}_1 \gamma_1^3. \tag{57}$$

Hence,

$$\frac{\partial}{\partial \bar{\theta}_1}(\bar{\theta}_1 \gamma_1) = \gamma_1 + \bar{\theta}_1^2 \gamma_1^3. \tag{58}$$

Similarly,

$$\begin{aligned} &\frac{\partial}{\partial \bar{\theta}_1} \left[\mu(\bar{\theta}_1 + \bar{\theta}_2 \cos \Delta\theta)\gamma_2\right] \\ &= \mu\gamma_2 + \mu(\bar{\theta}_1 + \bar{\theta}_2 \cos \Delta\theta) \frac{\partial \gamma_2}{\partial \bar{\theta}_1}, \end{aligned} \tag{59}$$

where

$$\frac{\partial \gamma_2}{\partial \bar{\theta}_1} = (\bar{\theta}_1 + \bar{\theta}_2 \cos \Delta\theta)\gamma_2^3. \tag{60}$$

Therefore,

$$\begin{aligned} A =& \gamma_1 + \bar{\theta}_1^2 \gamma_1^3 \\ &+ \mu \left[\gamma_2 + (\bar{\theta}_1 + \bar{\theta}_2 \cos \Delta\theta)^2 \gamma_2^3\right]. \end{aligned} \tag{61}$$

Evaluation of $B = \partial P_1/\partial \bar{\theta}_2$ Differentiating Eq. (39) with respect to $\bar{\theta}_2$ and applying the product rule gives

$$B = \mu \left[\cos(\theta_1 - \theta_2)\gamma_2 + (\bar{\theta}_1 + \bar{\theta}_2 \cos(\theta_1 - \theta_2)) \frac{\partial \gamma_2}{\partial \bar{\theta}_2} \right]. \tag{62}$$

Using

$$\frac{\partial \gamma_2}{\partial \bar{\theta}_2} = (\bar{\theta}_2 + \bar{\theta}_1 \cos(\theta_1 - \theta_2))\gamma_2^3, \tag{63}$$

the coefficient becomes

$$\begin{aligned} B =& \mu \Big[\cos(\theta_1 - \theta_2)\gamma_2 \\ &+ (\bar{\theta}_1 + \bar{\theta}_2 \cos(\theta_1 - \theta_2))(\bar{\theta}_2 + \bar{\theta}_1 \cos(\theta_1 - \theta_2))\gamma_2^3 \Big]. \end{aligned} \tag{64}$$

Evaluation of $D = \partial P_2/\partial \bar{\theta}_1$ Proceeding similarly, differentiation of Eq. (40) with respect to $\bar{\theta}_1$ yields

$$\begin{aligned} D =& \mu \Big[\cos(\theta_1 - \theta_2)\gamma_2 \\ &+ (\bar{\theta}_2 + \bar{\theta}_1 \cos(\theta_1 - \theta_2))(\bar{\theta}_1 + \bar{\theta}_2 \cos(\theta_1 - \theta_2))\gamma_2^3 \Big]. \end{aligned} \tag{65}$$

Comparison of Eqs. (64) and (65) immediately shows that

$$D = B, \tag{66}$$

reflecting the symmetry of the relativistic inertia matrix.

Evaluation of $E = \partial P_2/\partial \bar{\theta}_2$ Finally, differentiating Eq. (40) with respect to $\bar{\theta}_2$ gives

$$E = \mu \left[\gamma_2 + (\bar{\theta}_2 + \bar{\theta}_1 \cos(\theta_1 - \theta_2)) \frac{\partial \gamma_2}{\partial \bar{\theta}_2} \right]. \tag{67}$$

Substituting the expression for $\partial \gamma_2/\partial \bar{\theta}_2$ yields

$$E = \mu \Big[\gamma_2 + (\bar{\theta}_2 + \bar{\theta}_1 \cos(\theta_1 - \theta_2))^2 \gamma_2^3 \Big]. \tag{68}$$

The coefficients A, B, D, and E constitute the relativistic inertia matrix of the coupled double pendulum. These coefficients relate the generalized accelerations to the generalized forces and are used in the following subsection to derive the coupled equations of motion.

2.4.8 Construction of the Relativistic Equations of Motion

The generalized momenta derived in the previous subsections depend on both the generalized coordinates and generalized velocities. Consequently, their total time derivatives contain acceleration terms. Expanding the Euler–Lagrange equations,

$$\frac{dP_i}{dt} = F_i, \qquad (i = 1, 2), \tag{69}$$

and collecting the coefficients of the generalized accelerations gives the linear system

$$A\,\dot{\bar{\theta}}_1 + B\,\dot{\bar{\theta}}_2 = C, \tag{70}$$

$$D\,\dot{\bar{\theta}}_1 + E\,\dot{\bar{\theta}}_2 = F, \tag{71}$$

where the inertia coefficients A, B, D, and E were derived in the previous subsection.

The remaining coefficients are obtained from

$$C = F_1 - \frac{\partial P_1}{\partial \theta_1}\dot{\theta}_1 - \frac{\partial P_1}{\partial \theta_2}\dot{\theta}_2, \tag{72}$$

$$F = F_2 - \frac{\partial P_2}{\partial \theta_1}\dot{\theta}_1 - \frac{\partial P_2}{\partial \theta_2}\dot{\theta}_2. \tag{73}$$

The required angular derivatives of the generalized momenta are

$$\frac{\partial P_1}{\partial \theta_1} = -\mu\bar{\theta}_1\bar{\theta}_2 \sin\Delta\theta\,\gamma_2^3, \tag{74}$$

$$\frac{\partial P_1}{\partial \theta_2} = \mu\bar{\theta}_1\bar{\theta}_2 \sin\Delta\theta\,\gamma_2^3, \tag{75}$$

$$\frac{\partial P_2}{\partial \theta_1} = -\mu\bar{\theta}_1\bar{\theta}_2 \sin\Delta\theta\,\gamma_2^3, \tag{76}$$

$$\frac{\partial P_2}{\partial \theta_2} = \mu\bar{\theta}_1\bar{\theta}_2 \sin\Delta\theta\,\gamma_2^3. \tag{77}$$

Substituting these derivatives together with the generalized forces obtained in Eqs. (48) and (51) into Eqs. (72) and (73) yields

$$C = -(1+\mu)\alpha_1 \sin\theta_1 - \mu\bar{\theta}_1\bar{\theta}_2 \sin\Delta\theta\,\gamma_2, \tag{78}$$

and

$$F = -\mu\alpha_2 \sin\theta_2 + \mu\bar{\theta}_1\bar{\theta}_2 \sin\Delta\theta\,\gamma_2. \tag{79}$$

The coupled linear system represented by Eqs. (70) and (71) may be solved using Cramer's rule, giving the dimensionless angular accelerations

$$\dot{\bar{\theta}}_1 = \frac{CE - BF}{AE - BD}, \tag{80}$$

$$\dot{\bar{\theta}}_2 = \frac{AF - CD}{AE - BD}. \tag{81}$$

Recalling the definitions

$$\bar{\theta}_1 = \frac{L_1}{c}\dot{\theta}_1, \qquad \bar{\theta}_2 = \frac{L_2}{c}\dot{\theta}_2, \tag{82}$$

the physical equations of motion become

$$\ddot{\theta}_1 = \frac{c}{L_1}\frac{CE - BF}{AE - BD}, \tag{83}$$

$$\ddot{\theta}_2 = \frac{c}{L_2}\frac{AF - CD}{AE - BD}, \tag{84}$$

where

$$\mathcal{D} = AE - BD \tag{85}$$

is the determinant of the relativistic inertia matrix.

For completeness, the determinant may be written explicitly as

$$\begin{aligned}\mathcal{D} = &\left[\gamma_1 + \bar{\theta}_1^2\gamma_1^3 + \mu\left(\gamma_2 + (\bar{\theta}_1 + \bar{\theta}_2\cos\Delta\theta)^2\gamma_2^3\right)\right] \\ &\times \left[\mu\left(\gamma_2 + (\bar{\theta}_2 + \bar{\theta}_1\cos\Delta\theta)^2\gamma_2^3\right)\right] \\ &- \left[\mu\left(\cos\Delta\theta\,\gamma_2 + (\bar{\theta}_1 + \bar{\theta}_2\cos\Delta\theta)(\bar{\theta}_2 + \bar{\theta}_1\cos\Delta\theta)\gamma_2^3\right)\right]^2.\end{aligned} \tag{86}$$

Substituting the expressions for A, B, C, D, E, and F into Eqs. (83) and (84) gives the fully expanded relativistic equations of motion,

$$\begin{aligned}\ddot{\theta}_1 = \frac{c}{L_1}\frac{1}{\mathcal{D}}\Bigg\{&\Big[-(1+\mu)\alpha_1\sin\theta_1 - \mu\bar{\theta}_1\bar{\theta}_2\sin\Delta\theta\,\gamma_2\Big] \\ &\times \Big[\mu\left(\gamma_2 + (\bar{\theta}_2 + \bar{\theta}_1\cos\Delta\theta)^2\gamma_2^3\right)\Big] \\ &- \Big[\mu\left(\cos\Delta\theta\,\gamma_2 + (\bar{\theta}_1 + \bar{\theta}_2\cos\Delta\theta)(\bar{\theta}_2 + \bar{\theta}_1\cos\Delta\theta)\gamma_2^3\right)\Big] \\ &\times \Big[-\mu\alpha_2\sin\theta_2 + \mu\bar{\theta}_1\bar{\theta}_2\sin\Delta\theta\,\gamma_2\Big]\Bigg\},\end{aligned} \tag{87}$$

and

$$\begin{aligned}\ddot{\theta}_2 = \frac{c}{L_2}\frac{1}{\mathcal{D}}\Bigg\{&\left[\gamma_1 + \bar{\theta}_1^2\gamma_1^3 + \mu\left(\gamma_2 + (\bar{\theta}_1 + \bar{\theta}_2\cos\Delta\theta)^2\gamma_2^3\right)\right] \\ &\times \Big[-\mu\alpha_2\sin\theta_2 + \mu\bar{\theta}_1\bar{\theta}_2\sin\Delta\theta\,\gamma_2\Big] \\ &- \Big[-(1+\mu)\alpha_1\sin\theta_1 - \mu\bar{\theta}_1\bar{\theta}_2\sin\Delta\theta\,\gamma_2\Big] \\ &\times \Big[\mu\left(\cos\Delta\theta\,\gamma_2 + (\bar{\theta}_1 + \bar{\theta}_2\cos\Delta\theta)(\bar{\theta}_2 + \bar{\theta}_1\cos\Delta\theta)\gamma_2^3\right)\Big]\Bigg\}.\end{aligned} \tag{88}$$

The Lorentz factors are

$$\gamma_1 = \frac{1}{\sqrt{1-\bar{\theta}_1^2}}, \tag{89}$$

$$\gamma_2 = \frac{1}{\sqrt{1-\bar{\theta}_1^2-\bar{\theta}_2^2-2\bar{\theta}_1\bar{\theta}_2\cos\Delta\theta}}, \tag{90}$$

with

$$\Delta\theta = \theta_1 - \theta_2. \tag{91}$$

3 Numerical Methodology

3.1 Conversion to First-Order Differential Equations

The equations of motion derived in the previous section are two coupled nonlinear second-order differential equations. Since numerical integration methods such as the fourth-order Runge–Kutta (RK4) algorithm are formulated for first-order systems, these equations are first rewritten in state-space form.

The angular velocities are introduced as additional state variables,

$$\omega_1 = \dot{\theta}_1, \qquad \omega_2 = \dot{\theta}_2. \tag{92}$$

The corresponding angular accelerations can then be written as

$$\dot{\omega}_1 = f_1(\theta_1, \theta_2, \omega_1, \omega_2), \tag{93}$$

and

$$\dot{\omega}_2 = f_2(\theta_1, \theta_2, \omega_1, \omega_2), \tag{94}$$

where f_1 and f_2 represent the nonlinear functions obtained from the relativistic equations of motion.

The complete system may therefore be written as

$$\dot{\theta}_1 = \omega_1, \tag{95}$$
$$\dot{\omega}_1 = f_1(\theta_1, \theta_2, \omega_1, \omega_2), \tag{96}$$
$$\dot{\theta}_2 = \omega_2, \tag{97}$$
$$\dot{\omega}_2 = f_2(\theta_1, \theta_2, \omega_1, \omega_2). \tag{98}$$

The state of the system is represented by the vector

$$\mathbf{Y} = \begin{bmatrix} \theta_1 & \omega_1 & \theta_2 & \omega_2 \end{bmatrix}^T, \tag{99}$$

whose time evolution satisfies

$$\frac{d\mathbf{Y}}{dt} = \mathbf{F}(\mathbf{Y}, t), \tag{100}$$

where $\mathbf{F}$ contains the governing equations of motion. This first-order formulation is used throughout the numerical simulations described below.

3.2 Fourth-Order Runge–Kutta Method

The system of first-order differential equations was solved numerically using the classical fourth-order Runge–Kutta (RK4) method. This method is widely used because it provides good accuracy while remaining straightforward to implement for nonlinear ordinary differential equations [10, 11].

For a general first-order initial value problem,

$$\frac{d\mathbf{Y}}{dt} = \mathbf{F}(t, \mathbf{Y}), \qquad \mathbf{Y}(t_0) = \mathbf{Y}_0, \tag{101}$$

the RK4 algorithm advances the solution from t_n to $t_{n+1} = t_n + h$, where h is the integration time step. The numerical solution is updated according to

$$\mathbf{Y}_{n+1} = \mathbf{Y}_n + \frac{1}{6}\left(\mathbf{k}_1 + 2\mathbf{k}_2 + 2\mathbf{k}_3 + \mathbf{k}_4\right), \tag{102}$$

where

$$\mathbf{k}_1 = h\,\mathbf{F}(t_n, \mathbf{Y}_n), \tag{103}$$

$$\mathbf{k}_2 = h\,\mathbf{F}\left(t_n + \frac{h}{2}, \mathbf{Y}_n + \frac{\mathbf{k}_1}{2}\right), \tag{104}$$

$$\mathbf{k}_3 = h\,\mathbf{F}\left(t_n + \frac{h}{2}, \mathbf{Y}_n + \frac{\mathbf{k}_2}{2}\right), \tag{105}$$

$$\mathbf{k}_4 = h\,\mathbf{F}\left(t_n + h, \mathbf{Y}_n + \mathbf{k}_3\right). \tag{106}$$

At each time step, the four intermediate slopes are evaluated and combined using Eq. (102) to obtain the numerical solution. This procedure is repeated over the entire simulation interval to determine the angular positions and angular velocities of the system.

The simulations were carried out using a fixed integration time step, and the resulting numerical solutions were used to generate the time-series and phase-space plots presented in the next section.

3.3 Dimensionless Parameters

The governing equations were solved in dimensionless form using the parameters listed in Table 1. Unless otherwise stated, these values were used throughout the numerical simulations.

Table 1: Dimensionless parameters used in the numerical simulations.

Parameter	Value
Mass ratio, μ	1.0
Relativistic parameter, ε	0.2
Time step, $\Delta\tau$	0.005
Maximum integration time, $\tau_{\max}$	25

Three sets of initial conditions were considered to study different types of motion. These correspond to small-angle out-of-phase oscillations, small-angle in-phase oscillations, and large-angle nonlinear motion. The numerical solutions obtained for these cases are compared and discussed in the following section.

3.4 Numerical Implementation

The numerical algorithm was implemented in Python using a fixed-step fourth-order Runge–Kutta integrator. At each time step, the state vector

$$\mathbf{Y} = (\theta_1, \omega_1, \theta_2, \omega_2)^T \tag{107}$$

was updated according to the RK4 procedure described above.

The angular positions and angular velocities obtained from the numerical solution were then used to evaluate additional quantities, including the Lorentz factors of both pendulum masses. These quantities were subsequently used to generate the time-series plots, phase-space trajectories, and other results discussed in the next section.

All figures presented in this work were generated from the numerical solutions obtained using this computational procedure.

4 Results and Discussion

4.1 Verification of the Numerical Implementation

Before analysing the relativistic dynamics of the coupled double pendulum, the numerical implementation was checked to ensure that the governing equations were correctly implemented. The dimensionless equations derived in Section 2 were solved using the fourth-order Runge–Kutta method described in the previous section.

As a simple verification, the system was examined in the low-velocity limit, where relativistic effects become negligible. In this regime, the Lorentz factors approach unity, and the numerical solution agrees with the corresponding classical behaviour. This provides a useful consistency check for both the derived equations and their numerical implementation.

A fixed integration time step was used throughout all simulations, providing smooth numerical solutions over the chosen simulation interval. The verified implementation was then used to investigate the different dynamical cases presented in the following section.

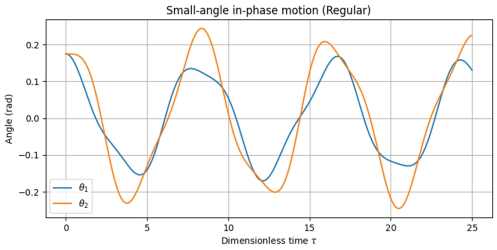
4.2 Small-Amplitude In-Phase Motion

To examine the behaviour of the relativistic model for small in-phase oscillations, simulations were carried out with both pendulum arms initially displaced by equal small angles in the same direction. Figure 3 compares the classical and relativistic responses obtained using the same initial conditions.

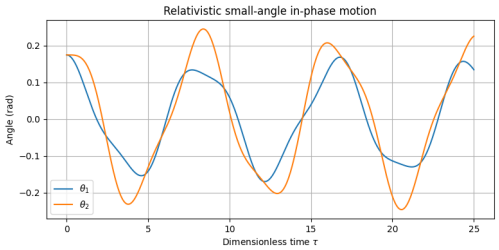
Figure 3(a) shows the classical solution reproduced using the formulation presented by D'Alessio [8]. The motion remains regular and periodic throughout the simulation. Figure 3(b) shows the corresponding relativistic solution obtained in the present work.

For both models, the pendulums initially oscillate in phase and continue to exhibit smooth, bounded motion over the entire simulation interval. As the motion progresses, the interaction between the two pendulums produces slight changes in their amplitudes and phase relationships. These changes are also present in the relativistic solution, where the velocity-dependent Lorentz factors introduce small corrections to the motion.

Although the relativistic effects are relatively weak for these small initial displacements, they produce noticeable differences when compared with the classical solution while preserving the overall periodic nature of the oscillations.



(a) Classical solution reproduced using the formulation of D'Alessio [8].



(b) Relativistic solution obtained in the present work.

Figure 3: Comparison of the time evolution of the angular displacements for the coupled double pendulum during small-amplitude in-phase motion. The classical and relativistic models are shown for the same initial conditions.

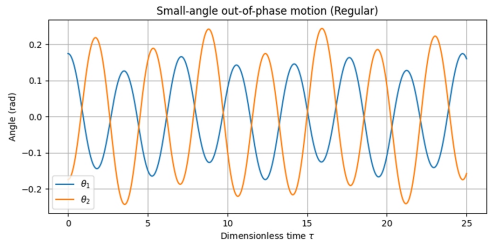
4.3 Small-Amplitude Out-of-Phase Motion

To examine the behaviour of the relativistic model for small oscillations, simulations were first performed using initial conditions corresponding to out-of-phase motion. Figure 4 compares the classical and relativistic responses obtained for the same initial conditions.

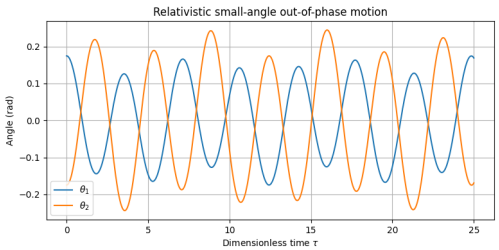
Figure 4(a) shows the classical solution, reproduced following the work of D'Alessio [8]. The motion remains regular and periodic throughout the simulation, providing a useful reference for comparison. Figure 4(b) shows the corresponding relativistic solution obtained in the present work.

Both models exhibit smooth and bounded oscillations over the entire simulation interval. The overall behaviour remains similar because the chosen initial conditions correspond to small angular displacements, where relativistic effects are expected to be relatively weak. Nevertheless, small differences in the amplitudes and phase relationships can be observed in the relativistic solution due to the velocity-dependent corrections introduced by the Lorentz factors.

These results indicate that the relativistic formulation preserves the regular oscillatory behaviour of the classical system while introducing subtle modifications to its dynamics.



(a) Classical model reproduced from the formulation of D'Alessio [8].



(b) Relativistic model obtained in the present work.

Figure 4: Comparison of the time evolution of the angular displacements for the coupled double pendulum during small-amplitude out-of-phase motion. The classical solution is shown alongside the corresponding relativistic solution for identical initial conditions.

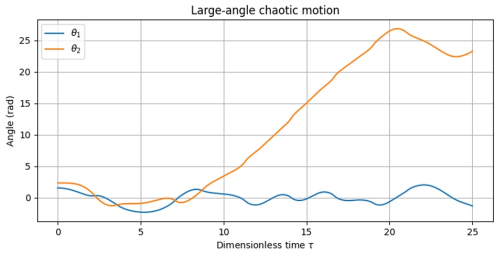
4.4 Large-Angle Dynamics

To investigate the behaviour of the system beyond the small-angle regime, simulations were performed using large initial angular displacements. Figure 5 compares the classical and relativistic responses obtained for the same initial conditions.

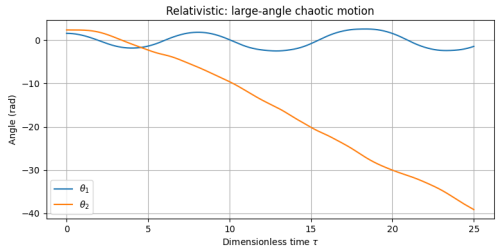
Figure 5(a) shows the classical solution reproduced using the formulation presented by D'Alessio [8], while Fig. 5(b) presents the corresponding relativistic solution obtained in the present work.

Compared with the small-angle cases, both models exhibit considerably more complex motion due to the strong nonlinear coupling between the two pendulum arms. The first pendulum continues to undergo bounded oscillations, whereas the second pendulum performs successive rotations, resulting in a continuous increase in its angular displacement. This behaviour indicates a transition from simple oscillatory motion to a regime where rotational motion becomes energetically possible.

The overall dynamical behaviour remains similar in both models. However, small differences can be observed in the relativistic solution as a result of the velocity-dependent corrections introduced by the Lorentz factors. These differences become more noticeable than in the small-angle cases because the pendulum velocities are larger during the motion.



(a) Classical solution reproduced using the formulation of D'Alessio [8].



(b) Relativistic solution obtained in the present work.

Figure 5: Comparison of the time evolution of the angular displacements for the coupled double pendulum with large initial angular displacements. The classical and relativistic solutions are shown for identical initial conditions.

4.5 Phase-Space Analysis

Phase-space portraits provide another way of examining the dynamics of the coupled pendulum system by showing the relationship between the angular displacement and the corresponding angular velocity. Unlike the time-domain plots, they illustrate how the state of the system evolves in phase space and help identify different types of motion.

Figure 6 presents the phase portraits obtained for the large-angle relativistic simulation. The phase portrait of the first pendulum, shown in Fig. 6(a), consists of a bounded orbit, indicating that the pendulum continues to undergo oscillatory motion despite the strong nonlinear coupling. The departure of the trajectory from a simple elliptical shape reflects the nonlinear nature of the system.

In contrast, the phase portrait of the second pendulum, shown in Fig. 6(b), exhibits a markedly different behaviour. As observed in the corresponding time-domain solution, the second pendulum undergoes successive rotations rather than remaining in bounded oscillatory motion. Consequently, the angular displacement changes continuously, producing an open trajectory in phase space instead of a closed orbit.

These phase portraits complement the time-domain results by clearly distinguishing the oscillatory motion of the first pendulum from the rotational behaviour of the second pendulum. Together, they illustrate the rich nonlinear dynamics exhibited by the relativistic coupled double pendulum for large initial angular displacements.

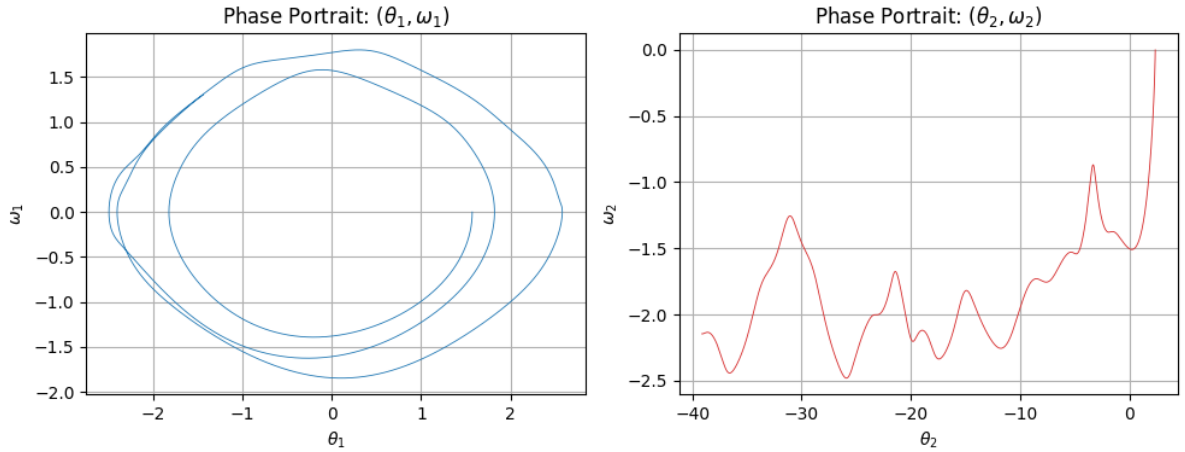


Figure 6: Phase portraits of the relativistic coupled double pendulum for the large-angle case: (a) phase portrait of the first pendulum (θ_1, ω_1) and (b) phase portrait of the second pendulum (θ_2, ω_2). The first pendulum exhibits bounded oscillatory motion, whereas the second pendulum displays rotational behaviour, resulting in an open trajectory in phase space.

4.6 Evolution of the Lorentz Factors

Figure 7 shows the time evolution of the Lorentz factors of the two pendulum masses during the large-angle relativistic simulation. Since the Lorentz factor depends directly on the velocity of each mass, it provides a convenient measure of the strength of relativistic effects throughout the motion.

The Lorentz factor of the first pendulum, γ_1, remains close to unity over the entire simulation interval, exhibiting only small periodic variations with a maximum value of approximately $\gamma_1 \approx 1.07$. This indicates that the velocity of the first pendulum remains relatively low, and therefore relativistic effects are modest throughout its motion.

In contrast, the Lorentz factor of the second pendulum, γ_2, displays significantly larger variations, reaching a maximum value of approximately $\gamma_2 \approx 1.39$. Several pronounced peaks are observed during the simulation, corresponding to intervals in which the second pendulum attains higher velocities while undergoing successive rotational motion. Between these peaks, the Lorentz factor decreases towards unity as the velocity is reduced.

The difference between the two curves reflects the distinct dynamical behaviour of the pendulum arms. While the first pendulum remains primarily oscillatory, the second pendulum experiences much larger velocity variations, leading to stronger relativistic effects. These results are consistent with the time-domain and phase-space analyses presented in the previous sections.

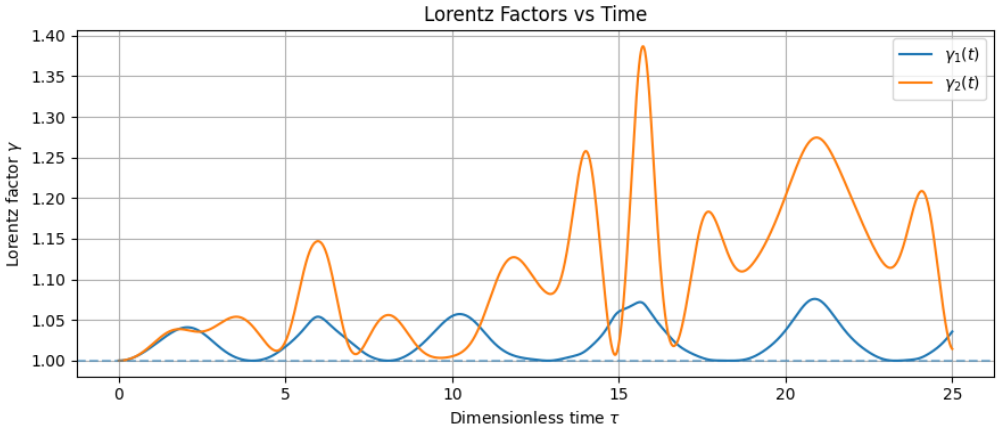


Figure 7: Time evolution of the Lorentz factors of the two pendulum masses during the large-angle relativistic simulation. The Lorentz factor of the first pendulum (γ_1) remains close to unity throughout the simulation, whereas the second pendulum (γ_2) exhibits larger fluctuations, reaching a maximum value of approximately 1.39 as higher velocities are attained during rotational motion.

4.7 Comparison Between Classical and Relativistic Dynamics

The numerical simulations show that the classical and relativistic models exhibit similar overall behaviour for small initial angular displacements. In both the in-phase and out-of-phase cases, the motion remains smooth, bounded, and predominantly periodic throughout the simulation interval. The relativistic solutions closely follow the corresponding classical responses, with only small differences in the amplitudes and phase relationships.

As the initial angular displacement increases, the differences between the two models become more noticeable. For the large-angle case, both formulations exhibit increasingly complex nonlinear motion, including the transition of the second pendulum from bounded oscillations to successive rotations. Although the overall dynamical behaviour remains similar, the relativistic solution displays modest deviations from the classical response as higher velocities are attained.

The evolution of the Lorentz factors provides further insight into these differences. The Lorentz factor of the first pendulum remains close to unity throughout the simulation, indicating relatively weak relativistic effects. In contrast, the second pendulum reaches considerably larger Lorentz factors during its rotational motion, reflecting the higher velocities attained by this pendulum and the increasing importance of relativistic corrections.

Overall, the numerical results demonstrate that the relativistic formulation reproduces the expected behaviour of the classical model in the low-velocity regime while introducing gradual velocity-dependent corrections as the motion becomes more energetic. The proposed model therefore provides a consistent extension of the classical coupled double pendulum for studying relativistic effects in nonlinear pendulum dynamics.

5 Conclusion

In this work, a relativistic formulation of the coupled double pendulum has been developed using the Lagrangian formalism within the framework of special relativity. Starting from the physical model, the governing equations of motion were derived systematically by incorporating relativistic kinetic energy while retaining the classical gravitational potential. The resulting nonlinear equations were subsequently transformed into a first-order state-space representation and solved numerically using the classical fourth-order Runge–Kutta method.

The numerical simulations demonstrate that the relativistic model reproduces regular oscillatory motion for small initial angular displacements while exhibiting increasingly complex dynamics for larger amplitudes. The computed Lorentz factors further illustrate that relativistic effects become progressively more significant as the velocities of the pendulum masses increase, particularly for the second pendulum.

The agreement of the relativistic model with the classical formulation in the low-velocity limit confirms the

consistency of the proposed approach. At the same time, the present formulation extends the classical coupled double pendulum by incorporating velocity-dependent inertial effects arising from special relativity.

The analytical framework developed in this work provides a foundation for future investigations of relativistic nonlinear dynamical systems. Possible extensions include unequal mass distributions, variable rod lengths, damping effects, external driving forces, and a more detailed investigation of chaotic dynamics using quantitative measures such as Lyapunov exponents and Poincaré sections.

Acknowledgements

All computational work presented in this paper was performed on the Sikkim University Brahmagupta High Performance Computing (HPC) facility. One of the authors (R.M.) acknowledges support from the Inter-University Centre for Astronomy and Astrophysics (IUCAA), Pune, through the Visiting Associate Programme.

The schematic illustrations of the simple and coupled double pendulum systems included in this paper were generated with the assistance of OpenAI's image generation tools and were subsequently reviewed, edited, and adapted by the authors for scientific presentation.

Acknowledgements

All computational work reported in this paper was carried out using the Brahmagupta High-Performance Computing (HPC) facility at Sikkim University. One of the authors, Rupak Mukherjee gratefully acknowledges the support provided by the Inter-University Centre for Astronomy and Astrophysics (IUCAA), Pune, through its Visiting Associate Programme.

AI Disclosure Statement

In preparing this work, the authors used Google Gemini to assist in generating one illustrative figure and polishing the overall English language of the manuscript. All scientific observations, computational work, analyses, and results were independently carried out and verified by the authors. The authors subsequently reviewed and revised the content as necessary and accept full responsibility for the final published work.

References

[1] Herbert Goldstein, Charles Poole, and John Safko, Classical Mechanics, 3rd ed. (Pearson, 2002).

[2] L. D. Landau and E. M. Lifshitz, Mechanics, 3rd ed. (Butterworth-Heinemann, 1976).

[3] John R. Taylor, Classical Mechanics, (University Science Books, 2005).

[4] Steven H. Strogatz, Nonlinear Dynamics and Chaos, 2nd ed. (CRC Press, 2018).

[5] Edward Ott, Chaos in Dynamical Systems, 2nd ed. (Cambridge University Press, 2002).

[6] Troy Shinbrot, Celso Grebogi, Jack Wisdom, and James A. Yorke, "chaos in a double pendulum", American Journal of Physics 60, 491–499 (1992).

[7] R. Levien and S. Tan, "Double pendulum: An experiment in chaos", American Journal of Physics, (1993).

[8] Serge D'Alessio, "An analytical, numerical and experimental study of the double pendulum", European Journal of Physics 44, 015002 (2023).

[9] Wolfgang Rindler, Introduction to Special Relativity, (Oxford University Press, 1991).

[10] Richard L. Burden and J. Douglas Faires, Numerical Analysis, 8th ed. (Brooks/Cole, 2005).

[11] William H. Press, Saul A. Teukolsky, William T. Vetterling, and Brian P. Flannery, Numerical Recipes, 3rd ed. (Cambridge University Press, 2007).